HHS Public Access

Author manuscript

J Neuroophthalmol. Author manuscript; available in PMC 2019 September 01.

Published in final edited form as:

J Neuroophthalmol. 2018 September ; 38(3): 292–298. doi:10.1097/WNO.0000000000000580.

Altered macular microvasculature in mild cognitive impairment and Alzheimer disease

Hong Jiang, MD, PhD[1,2], **Yantao Wei, MD, PhD**[1,3], **Yingying Shi, MD**[1], **Clinton B. Wright, MD, MS**[2], **Xiaoyan Sun, MD, PhD**[2], **Giovanni Gregori, PhD**[1], **Fang Zheng, MD**[1], **Elizabeth Anne Vanner, PhD**[1,4], **Byron L. Lam, MD**[1], **Tatjana Rundek, MD, PhD**[2], and **Jianhua Wang, MD, PhD**[1]

[1]Department of Ophthalmology, Bascom Palmer Eye Institute, University of Miami Miller School of Medicine, Miami, FL, USA

[2]Evelyn F. McKnight Brain Institute, Department of Neurology, University of Miami Miller School of Medicine, Miami, FL, USA

[3]State Key laboratory of Ophthalmology, Zhongshan Ophthalmic Centre, Sun Yat-sen University, Guangzhou, Guangdong, 510060, China

[4]BioStatistics Center, Bascom Palmer Eye Institute, University of Miami Miller School of Medicine, Miami, FL, USA

[*]Corresponding Author: Hong Jiang, MD, PhD, Mailing address: Bascom Palmer Eye Institute, University of Miami, Miller School of Medicine, 1638 NW 10th Avenue, McKnight Building - Room 202A, Miami, FL, 33136., Tel: (305) 482-5010, hjiang@med.miami.edu.

Statement of Authorship

Category 1:

a. Conception and design

Hong Jiang, Clinton B. Wright, Tatjana Rundek, Jianhua Wang

b. Acquisition of data

Yantao Wei, Yingying Shi, Clinton B. Wright, XiaoYan Sun, Giovanni Gregori, Fang Zheng, Hong Jiang, Jianhua Wang, Byron L Lam

c. Analysis and interpretation of data

Hong Jiang, Yantao Wei, Yingying Shi, Clinton B. Wright, Xiaoyan Sun, Giovanni Gregori, Fang Zheng, Elizabeth Ann Vanner

Category 2:

a. Drafting the manuscript

Hong Jiang, Jianhua Wang

b. Revising it for intellectual content

Clinton B. Wright, Giovanni Gregori, Elizabeth Anne Vanner, Byron L Lam, Tatjana Rundek, Hong Jiang, Jianhua Wang

Category 3:

a. Final approval of the completed manuscript

Yantao Wei, Yingying Shi, Clinton B. Wright, XiaoYan Sun, Giovanni Gregori, Fang Zheng, Hong Jiang, Jianhua Wang, Byron L Lam

Financial Disclosures: Dr. Gregori has research support from Carl Zeiss Meditec. There are no conflicting relationship exists for any other authors.

Abstract

Purpose—To analyze the macular microvascular network in mild cognitive impairment (MCI) and Alzheimer disease (AD).

Methods—Twelve AD patients and 19 MCI patients were recruited together with 21 cognitively normal (CN) controls with a similar range of ages. Optical coherence tomography angiography (OCTA) was used to image the retinal microvascular network at the macular region including retinal vascular network (RVN), superficial vascular plexus (SVP), and deep vascular plexus (DVP). Fractal analysis (box counting, D_{box}) representing the microvascular density was performed in different annular zones and quadrantal sectors. The macular ganglion cell-inner plexiform layer (GC-IPL) thickness was measured using Zeiss OCT. The relationship between the retinal microvasculature and clinical manifestations was analyzed.

Results—AD patients had lower densities of RVN, SVP and DVP in the annulus, from 0.6 to 2.5 mm in diameter ($P < 0.05$) in comparison to controls. MCI patients had lower density of DVP in the superior nasal quadrant ($P < 0.05$) than that of the controls. There were no significant differences of GC-IPL thickness among groups ($P > 0.05$). There was a trend of vascular density loss from control to MCI then AD ($P < 0.05$). Retinal microvascular density of DVP was correlated to GC-IPL thickness ($P < 0.05$) in AD patients, but not in MCI patients and controls.

Conclusions—AD patients had less density of retinal microvascular networks than controls. Our findings suggest the presence of retinal microvascular dysfunction in AD.

Keywords

Alzheimer’s disease (AD); retinal vascular network (RVN); superficial vascular plexus (SVP); deep vascular plexus (DVP); optical coherence tomography angiography (OCTA); ganglion cell - inner plexiform layer (GCIPL)

Extensive evidence indicates that the vascular factors contributes to cerebral neurodegeneration in AD (1). Multiple vascular risk factors were found to be related to AD in large scale epidemiological studies (2,3), and control of these vascular risk factors may reduce the likelihood of developing AD (4–6). Global and focal cerebral hypoperfusion measured by transcranial Doppler, single-photon emission computed tomography and arterial spin MRI is not only evident in AD, but also exists in mild cognitive impairment (MCI) (7,8). Longitudinal studies have demonstrated that decreased cerebral perfusion in MCI can predict progression to AD (9). In comparison to cognitively normal (CN) controls of similar ages, microscopic pathologic studies showed significant structural changes of the cerebral vasculature in AD, such as loose capillary density, capillary kinking, looping, and twisting (10,11). Cerebral amyloid angiopathy is one of the major pathologic changes in AD besides amyloid plaques and neurofibrillary tangles (12). Despite the evidence suggesting that vascular impairment plays a role in the pathogenesis of AD, it is unknown whether vascular alterations precede and contribute to neural death or whether they are the bystander effect from decreased metabolic demand. The lack of data is due to the difficulty in visualizing and assessing the cerebral microvasculature in vivo.

Similar to the brain, the retina has a highly isolated and protected vascular system, and shares similar physiological and anatomical features with the brain (13,14). The transparent ocular media enables a noninvasive evaluation of the retinal vasculature. Epidemiologic studies using fundus photography have demonstrated less complex retinal vasculature, and smaller, more tortuous retinal vessels in patients with AD compared to CN controls (15–17). In addition, the loss of ganglion cells appears to correlate with cerebral atrophy (18).

With advancements in imaging techniques, microvascular networks that are invisible on fundus photos can be noninvasively imaged (19). Optical coherence tomography angiography (OCTA) can image both the superficial and deep retinal microvascular plexuses, which reflect retinal perfusion (19). Compared to previous investigations on the retinal vasculature using fundus images (15,20), OCTA enables visualization of the retinal microvascular network, including the capillary network, at the micrometer level. Studying the retinal microvasculature (pre-capillary arterioles, capillaries, post-capillary venules) and retinal neurodegeneration may provide insight into the role of vascular dysfunction in the pathogenesis of AD. The goal of our study was to characterize retinal microvascular network and its relation to retinal neuronal structure in patients with MCI and AD.

METHODS

The study was approved by the institutional review board for human research at the University of Miami, and signed informed consent was obtained from each subject. AD and MCI patients were recruited from the McKnight Brain Registry and referred from the Division of Cognitive Disorders at the University of Miami to the neuro-ophthalmology clinic at the Bascom Palmer Eye Institute. A group consensus conference that included neurologists, psychiatrists, and neuropsychologists discussed and confirmed the diagnoses of AD (21) and MCI (22) based on National Institute on Aging–Alzheimer's Association (NIA-AA) criteria. The disease duration was calculated from the date of symptoms onset. All subjects were treated in accordance with the Tenets of the Declaration of Helsinki. We excluded patients with high refractive errors of more than +6.0 or −6.0 diopters (due to the limit of the imaging device) or with any ocular disease, such as age-related macular degeneration, diabetic retinopathy, cystic macular edema, dense cataracts or corneal disease. To ensure image quality, the cutoff of the signal strength of optical coherence tomography (OCT) scan was set to be 5, which is likely the minimal signal strength for OCT measurements of macular, optic nerve head and retinal nerve fiber layer parameters (23). Patients with a history of stroke, coagulopathy, uncontrolled hypertension, and uncontrolled diabetes also were excluded. The CN controls were cognitively normal individuals who fit the same inclusion and exclusion criteria. Their Mini-Mental State Examination (MMSE) was done by trained and qualified neurologist (H.J.) or research associates (Y.S. & Y.W.).

Retinal microvasculature was acquired using Zeiss Angioplex™ OCTA (Carl Zeiss Meditec, Dublin, CA) (19), covering a retina area of 3×3 mm^2 centered on the fovea. There are two layers of the interconnecting retinal capillary network: the superficial vascular plexus (SVP), located in the retinal nerve fiber and ganglion cell layers, containing arterioles, venules, and capillaries, and the deep vascular plexus (DVP) located in the inner nuclear and outer plexiform layers which contains mainly capillary-sized vessels (Fig. 1) (24). The total retinal

vascular network (RVN) is defined as the vasculature in the retina including both SVP and DVP (19). The enface images of RVN, SVP and DVP were exported. These images were analyzed using custom software including separation of large and small vessels, partition of quadrantal sectors and annular zones, and fractal analysis of the processed images (25,26). Briefly, images with a size of 245 × 245 pixels were resized to 1,024 × 1,024 pixels for vessel segmentation (27,28). The segmentation removed the large vessels from the microvascular network and extracted the microvascular network using image processing procedures, such as inverting, equalizing and removing background noise and non-vessel structures to create a binary image. Vessels with a diameter ≥ 25 μm were defined as large vessels and separated from the remaining vessels, which were considered as microvessels (25,26). This procedure also was used to eliminate the shadow graphic projection artifact of the large vessels in the SVP, which was projected onto the DVP (29).

The binary images of the extracted microvessels were skeletonized. The center of the foveal avascular zone (FAZ) was located, and the center of the FAZ was used for all the subsequent partitions. As in our previous studies (25,26), a disc with a diameter of 0.6 mm (which roughly represents the avascular zone) was not used in the analysis. The area between circles with diameters of 0.6 mm to 2.5 mm was defined as the annular zone (Fig. 2). The annular zone was then divided into four quadrantal sectors, named the superior temporal (ST), inferior temporal (IT), superior nasal (SN) and inferior nasal (IN). The annular zone was also divided into 6 thin annuli with a width of ~0.16 mm due to the uneven distribution of retinal ganglion cells and corresponding vascular supply (30). Due to the symmetric structure of the retina between the left and right eyes, the results of the nasal or temporal sectors of both the left and right eyes were averaged.

Standard OCT scans were used to quantify the thickness of macular ganglion cell-inner plexiform layer (GC-IPL) imaged using Zeiss 200 × 200 macular cube scan protocol (Fig. 3) (31). Measurements of GC-IPL thickness were obtained whole annulus with removal of the center elliptic zone and 6 sectors of the annulus, including the superior temporal (ST), superior (S), superior nasal (SN), inferior nasal (IN), inferior (I) and inferior temporal (IT) sectors of the annulus.

One eye of each patient or CN control was imaged. The right eye was the first choice for imaging. The left eye was selected if the right eye did not meet the eligibility criteria. Patients and CN controls were asked to avoid large meals and to not drink alcohol or coffee before ophthalmic imaging. They were also advised to avoid physical exercise for 24 hours prior to the study.

Fractal analysis was performed in each sector or annular zone using the box counting method with the fractal analysis toolbox (TruSoft Benoit Pro 2.0, TruSoft International, Inc., St. Petersburg, FL) (25,26). The fractal dimension (D_{box}) was obtained, representing the vessel density in each zone.

Analyzed using SAS (SAS Institute, Cary NC, ver. 9.4), analysis of covariance (ANCOVA) was used to test for a trend from AD to MCI to control. Spearman rank-order correlation was used to evaluate the relationship among the parameters and the Spearman's correlation

coefficient (ρ) is reported. Chi-Square test was used to test the confounding factors. A result of $P < 0.05$ was considered significantly different

RESULTS

The baseline characteristics of the patients are listed in Table E1. There were no significant differences in demographics and vascular risk factors among the groups ($P > 0.05$). The AD patient cohort, as expected, had a significantly worse MMSE compared to the MCI group ($P < 0.01$). Large vessels and microvessels were clearly visualized in the OCTA images in both SVP and RVN (Fig. 4). The majority of vessels in the DVP were small vessels. The large vessels in the DVP were projection artifacts of the large vessels in SVP (29). Compared to the CN controls, the large vessels in AD and MCI patients appeared to have similar densities. Compared to controls, AD patients had lower densities of RVN, SVP and DVP in the annulus from 0.6 to 2.5 mm in diameter (Fig. E1, $P < 0.05$). Quadrantal analysis showed AD had lower vessel densities in all quadrants of RVN, ST quadrant of SVP, and ST and IN quadrants of DVP (Fig. E1, $P < 0.05$). Analysis of thin annuli showed AD had a lower density of RVN in annuli C2 – C6 (from 0.92 to 2.5 mm) (Fig. E2, $P < 0.05$). In addition, the annuli C3–4 (from 1.55 to 1.87 mm) showed a lower density of SVP and DVP in AD (Fig. E2, $P < 0.05$), compared to controls.

In MCI patients, the density of retinal microvessels of DVP in the SN quadrant was significantly lower (Fig. E1, $P < 0.05$), compared to controls. Thin annulus analysis showed that the density of DVP in annuli C1–6 (from 0.60 to 2.5 mm) was significantly lower (Fig. E2, $P < 0.05$), compared to controls.

GC-IPL thickness was measured as the averaged values of the whole annulus and 6 sectors. There were no significant differences among groups in the average values and sectors (Fig. E3, $P > 0.05$). The ANCOVA results indicated that there was a statistically significant trend with higher density in the control patients compared to the MCI patients, and higher density in the MCI patients compared to the AD patients for all RVN variables except the C1 (innermost) annular zone. The same statistically significant trend was observed in the SVP whole annulus, superior temporal quadrant, and the C3 and C4 annular zones, and in the DVP whole annulus, superior temporal and inferior nasal quadrants, and the C3 and C4 annular zones. No significant trends were observed in the GC-IPL thickness of the whole annulus or the 6 sectors.

In AD patients, the microvascular density in the DVP was related to the GC-IPL annular thickness (Fig. E4, $\rho = 058$, $P < 0.05$). None of microvascular measurements was related to disease duration and MMSE ($P > 0.05$). In MCI patients, none of the microvascular measurements was related to the GCIPL annular thickness (Fig. E5, $P > 0.05$) and disease duration ($P > 0.05$). However, the microvascular network density in the retinal microvascular network was positively related to MMSE in MCI patients ($\rho = 0.49$, $P < 0.05$). In the CN controls, none of the microvascular measurements was related to the GCIPL thickness ($P > 0.05$).

DISCUSSION

The loss of retinal microvascular density in AD patients found in our study indicates the impairment of retinal microvasculature. The alterations that we detected support the hypothesis that vascular impairment resulting in tissue hypoperfusion may contribute to disease onset and progression and may echo the findings in the brain (7–9). The trend of retinal microvascular loss from MCI to AD may indicate retinal vascular impairment during disease progression which may contribute to the potential conversion from MCI to AD. Interestingly, the relation between the impaired macular microvasculature and macular ganglion cell layer thickness was not established, which may be due to the different regions of interest that we measured. The vessel density was measured in a 3×3 mm^2 while the GC-IPL thickness was measured in a 6×6 mm^2 (analyzed in an ellipsoidal area). In addition, the macular RNFL (axonal fibers) was not analyzed. Further studies investigating the relationship between the macular microvasculature and macular RNFL are needed for better understanding the effect of the impaired macular microvasculature on retinal neurodegeneration. As the window to the brain, monitoring retinal microvasculature may add insightful information in the pathophysiology of AD, particularly the role of vascular contribution to neurodegeneration in disease progression and treatment efficacy. Monitoring retinal microvasculature in addition to retinal structural measurements may prove valuable in better understanding the mechanism of cerebral neural loss in AD.

While there were no correlations between retinal microvasculature and GC-IPL thickness in MCI group and CN control group, the correlation between the loss of retinal microvasculature in DVP and the GC-IPL thinning was established in AD group. Although the relation ($\rho = 0.55$) between SVP and GCIPL did not reach the significant level, but was similar to the relation ($\rho = 0.58$) between DVP and GC-IPL. The SVP is located in the retinal nerve fiber and ganglion cell layers, while the DVP is located in the inner nuclear and outer plexiform layers. One possible explanation could be that DVP primarily is composed of capillaries which may be affected earlier and to a greater extent than SVP which is composed of relatively larger vessels (pre-capillary arterioles, capillaries and post-capillary venules). Future studies with a large sample size may establish the relation between SVP and GC-IPL.

MMSE has been reported to not be sensitive enough to differentiate MCI from AD because many factors influence cognitive tests (32,33). This also may explain why we did not find correlations between the MMSE score and retinal microvascular alterations in patients with AD. Interestingly, a positive relation between the RVN and MMSE was found in MCI, and further large sample studies are needed to validate this relationship.

The OCTA angiogram shows the details of the retinal vasculature, including large vessels that are visible on fundus photos and microvessels that are not visible on fundus photos (19). Removal of the large vessels helps analyze the microvascular network (25–27). Our automated quantitative software for evaluating the capillary network imaged by OCTA was evolved from our previous analysis of the microvascular network obtained from the Retinal Function Imager (RFI) and has the features with detailed partitions and large vessel removal in addition to fractal analyses (27,28). The repeatability tests of the data acquired using

OCTA were confirmed to be valid (25,26). Careful analysis of the retinal microvasculature may be the key for revealing early signs of microvascular impairment in MCI and AD. The fractal dimension of the annulus (0.6 – 2.5 mm) of the microvascular network is ~1.75 – 1.78 in both the SVP and DVP of healthy young adults (25,26). In the present study, the fractal dimension in the elderly CN controls was ~1.74 in SVP and ~1.73 in DVP, which is slightly lower than previously reported, likely due to normal aging. The disease process may further induce microvascular network loss on top of the normal aging by about 0.05 (fractal dimension) in patients with AD and 0.03 in patients with MCI. In addition to the overall analysis of the retinal microvasculature, detailed partitioning may add another dimension in understanding early disease changes. When only the total annulus was analyzed, sectorial changes may be missed. This may be due to the non-uniform distribution of retinal ganglion cells and corresponding vascular supply (30). The density of microvasculature was highest from 0.5 mm to 1.25 mm from the fovea per our previous study (25).

There are limitations to the present study. First our small sample size, especially of the AD group, may have been a factor in not being able to show significant changes in all quadrants and annuli. However, significant changes in certain annuli and sectors were determined in AD, indicating that analyzing retinal microvascular network is sensitive for detecting the changes. Second, age matching is another limitation of our study. The mean age was 73.3 years in AD group, 69.6 years in MCI group, and 67.6 years in CN control group with a trend of younger age in the MCI and CN group. Although statistically there were no significant differences of ages among groups, the slight difference in the mean age (~6 yrs) may contribute to the difference of macular vessel density of the AD group in comparison with the CN group. Third, we studied the correlations of retinal microvascular alterations with GC-IPL, disease duration, and MMSE but not with other clinical or neuroimaging features of AD and MCI. Fourth, the cross-sectional nature of our study cannot provide information about temporal causality of vascular alterations and neurodegeneration. Future longitudinal studies are needed. Lastly, the analyses of adjacent tissue sections cannot be considered statistically independent, since the microvasculature of adjacent tissue sections are more likely to be similar than the microvasculature of non-adjacent tissue sections. Yet this does not compromise the statistical validity of our analyses because, within all of our analyses, the individual data (eyes) were independent, and this is what is required by the assumptions of statistical tests.

In conclusion, AD patients had less density of the retinal microvascular networks than controls. The trend of retinal microvascular loss may indicate progressive retinal vascular impairment during disease progression.

Supplementary Material

Refer to Web version on PubMed Central for supplementary material.

Acknowledgments

Grant/financial support: Grant/financial support: Supported by North American Neuro-ophthalmology Society, McKnight Brain Institute, NIH Center Grant P30 EY014801, and a grant from Research to Prevent Blindness (RPB). Dr. Gregori has research support from Carl Zeiss Meditec.

References

1. de la Torre JC. Vascular risk factors: a ticking time bomb to Alzheimer's disease. Am J Alzheimers Dis Other Demen. 2013; 28:551–559. [PubMed: 23813612]
2. Ott A, Stolk RP, van HF, Pols HA, Hofman A, Breteler MM. Diabetes mellitus and the risk of dementia: The Rotterdam Study. Neurology. 1999; 53:1937–1942. [PubMed: 10599761]
3. Hofman A, Ott A, Breteler MM, Bots ML, Slooter AJ, van HF, van Duijn CN, Van BC, Grobbee DE. Atherosclerosis, apolipoprotein E, and prevalence of dementia and Alzheimer's disease in the Rotterdam Study. Lancet. 1997; 349:151–154. [PubMed: 9111537]
4. de la Torre JC. Vascular risk factor detection and control may prevent Alzheimer's disease. Ageing Res Rev. 2010; 9:218–225. [PubMed: 20385255]
5. de la Torre JC. Cerebral hemodynamics and vascular risk factors: setting the stage for Alzheimer's disease. J Alzheimers Dis. 2012; 32:553–567. [PubMed: 22842871]
6. de la Torre JC. A turning point for Alzheimer's disease? Biofactors. 2012; 38:78–83. [PubMed: 22422426]
7. Ruitenberg A, den HT, Bakker SL, van Swieten JC, Koudstaal PJ, Hofman A, Breteler MM. Cerebral hypoperfusion and clinical onset of dementia: the Rotterdam Study. Ann Neurol. 2005; 57:789–794. [PubMed: 15929050]
8. Austin BP, Nair VA, Meier TB, Xu G, Rowley HA, Carlsson CM, Johnson SC, Prabhakaran V. Effects of hypoperfusion in Alzheimer's disease. J Alzheimers Dis. 2011; 26(Suppl 3):123–133. [PubMed: 21971457]
9. Park KW, Yoon HJ, Kang DY, Kim BC, Kim S, Kim JW. Regional cerebral blood flow differences in patients with mild cognitive impairment between those who did and did not develop Alzheimer's disease. Psychiatry Res. 2012; 203:201–206. [PubMed: 22980226]
10. Buee L, Hof PR, Delacourte A. Brain microvascular changes in Alzheimer's disease and other dementias. Ann N Y Acad Sci. 1997; 826:7–24. [PubMed: 9329677]
11. de la Torre JC. Hemodynamic consequences of deformed microvessels in the brain in Alzheimer's disease. Ann N Y Acad Sci. 1997; 826:75–91. [PubMed: 9329682]
12. Knight MJ, McCann B, Kauppinen RA, Coulthard EJ. Magnetic Resonance Imaging to Detect Early Molecular and Cellular Changes in Alzheimer's Disease. Front Aging Neurosci. 2016; 8:139. [PubMed: 27378911]
13. Patton N, Aslam T, MacGillivray T, Pattie A, Deary IJ, Dhillon B. Retinal vascular image analysis as a potential screening tool for cerebrovascular disease: a rationale based on homology between cerebral and retinal microvasculatures. J Anat. 2005; 206:319–348. [PubMed: 15817102]
14. London A, Benhar I, Schwartz M. The retina as a window to the brain-from eye research to CNS disorders. Nat Rev Neurol. 2013; 9:44–53. [PubMed: 23165340]
15. Cheung CY, Ong YT, Ikram MK, Ong SY, Li X, Hilal S, Catindig JA, Venketasubramanian N, Yap P, Seow D, Chen CP, Wong TY. Microvascular network alterations in the retina of patients with Alzheimer's disease. Alzheimers Dement. 2014; 10:135–142. [PubMed: 24439169]
16. Williams MA, McGowan AJ, Cardwell CR, Cheung CY, Craig D, Passmore P, Silvestri G, Maxwell AP, McKay GJ. Retinal microvascular network attenuation in Alzheimer's disease. Alzheimers Dement (Amst). 2015; 1:229–235. [PubMed: 26634224]
17. Frost S, Kanagasingam Y, Sohrabi H, Vignarajan J, Bourgeat P, Salvado O, Villemagne V, Rowe CC, Macaulay SL, Szoeke C, Ellis KA, Ames D, Masters CL, Rainey-Smith S, Martins RN. AIBL Research Group. Retinal vascular biomarkers for early detection and monitoring of Alzheimer's disease. Transl Psychiatry. 2013; 3:e233. [PubMed: 23443359]
18. Cheung CY, Ong YT, Hilal S, Ikram MK, Low S, Ong YL, Venketasubramanian N, Yap P, Seow D, Chen CL, Wong TY. Retinal ganglion cell analysis using high-definition optical coherence tomography in patients with mild cognitive impairment and Alzheimer's disease. J Alzheimers Dis. 2015; 45:45–56. [PubMed: 25428254]
19. Rosenfeld PJ, Durbin MK, Roisman L, Zheng F, Miller A, Robbins G, Schaal KB, Gregori G. ZEISS Angioplex Spectral Domain Optical Coherence Tomography Angiography: Technical Aspects. Dev Ophthalmol. 2016; 56:18–29. [PubMed: 27023249]

20. Cheung CY, Ong YT, Ikram MK, Chen C, Wong TY. Retinal microvasculature in Alzheimer's disease. J Alzheimers Dis. 2014; 42(Suppl 4):S339–S352. [PubMed: 25351108]
21. McKhann GM, Knopman DS, Chertkow H, Hyman BT, Jack CR Jr, Kawas CH, Klunk WE, Koroshetz WJ, Manly JJ, Mayeux R, Mohs RC, Morris JC, Rossor MN, Scheltens P, Carrillo MC, Thies B, Weintraub S, Phelps CH. The diagnosis of dementia due to Alzheimer's disease: recommendations from the National Institute on Aging-Alzheimer's Association workgroups on diagnostic guidelines for Alzheimer's disease. Alzheimers Dement. 2011; 7:263–269. [PubMed: 21514250]
22. Albert MS, DeKosky ST, Dickson D, Dubois B, Feldman HH, Fox NC, Gamst A, Holtzman DM, Jagust WJ, Petersen RC, Snyder PJ, Carrillo MC, Thies B, Phelps CH. The diagnosis of mild cognitive impairment due to Alzheimer's disease: recommendations from the National Institute on Aging-Alzheimer's Association workgroups on diagnostic guidelines for Alzheimer's disease. Alzheimers Dement. 2011; 7:270–279. [PubMed: 21514249]
23. Samarawickrama C, Pai A, Huynh SC, Burlutsky G, Wong TY, Mitchell P. Influence of OCT signal strength on macular, optic nerve head, and retinal nerve fiber layer parameters. Invest Ophthalmol Vis Sci. 2010; 51:4471–4475. [PubMed: 20445116]
24. Kur J, Newman EA, Chan-Ling T. Cellular and physiological mechanisms underlying blood flow regulation in the retina and choroid in health and disease. Prog Retin Eye Res. 2012; 31:377–406. [PubMed: 22580107]
25. Li M, Yang Y, Jiang H, Gregori G, Roisman L, Zheng F, Ke B, Qu D, Wang J. Retinal microvascular network and microcirculation assessments in high myopia. Am J Ophthalmol. 2017; 174:56–67. [PubMed: 27818204]
26. Yang Y, Wang J, Jiang H, Yang X, Feng L, Hu L, Wang L, Lu F, Shen M. Retinal Microvasculature Alteration in High Myopia. Invest Ophthalmol Vis Sci. 2016; 57:6020–6030. [PubMed: 27820633]
27. Jiang H, Delgado S, Liu C, Rammohan KW, DeBuc DC, Lam BL, Wang J. In Vivo Characterization of Retinal Microvascular Network in Multiple Sclerosis. Ophthalmology. 2016; 123:437–438. [PubMed: 26299696]
28. Jiang H, DeBuc DC, Rundek T, Lam BL, Wright CB, Shen M, Tao A, Wang J. Automated segmentation and fractal analysis of high-resolution non-invasive capillary perfusion maps of the human retina. Microvasc Res. 2013; 89:172–175. [PubMed: 23806780]
29. Zhang M, Hwang TS, Campbell JP, Bailey ST, Wilson DJ, Huang D, Jia Y. Projection-resolved optical coherence tomographic angiography. Biomed Opt Express. 2016; 7:816–828. [PubMed: 27231591]
30. Curcio CA, Allen KA. Topography of ganglion cells in human retina. J Comp Neurol. 1990; 300:5–25. [PubMed: 2229487]
31. Mwanza JC, Durbin MK, Budenz DL, Girkin CA, Leung CK, Liebmann JM, Peace JH, Werner JS, Wollstein G. Profile and predictors of normal ganglion cell-inner plexiform layer thickness measured with frequency-domain optical coherence tomography. Invest Ophthalmol Vis Sci. 2011; 52:7872–7879. [PubMed: 21873658]
32. Tsoi KK, Chan JY, Hirai HW, Wong SY, Kwok TC. Cognitive Tests to Detect Dementia: A Systematic Review and Meta-analysis. JAMA Intern Med. 2015; 175:1450–1458. [PubMed: 26052687]
33. Arevalo-Rodriguez I, Smailagic N, Roque IF, Ciapponi A, Sanchez-Perez E, Giannakou A, Pedraza OL, Bonfill CX, Cullum S. Mini-Mental State Examination (MMSE) for the detection of Alzheimer's disease and other dementias in people with mild cognitive impairment (MCI). Cochrane Database Syst Rev. 2015:CD010783. [PubMed: 25740785]

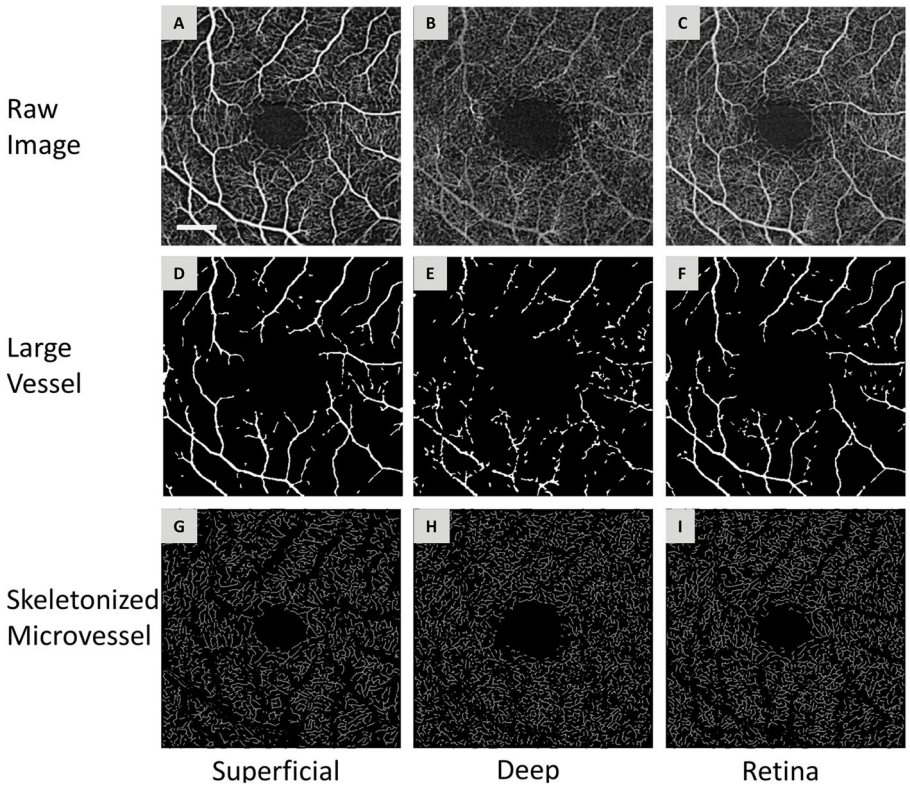

Figure 1. Segmentation of OCTA images

The superficial (A) and deep (B) vascular plexuses and retinal vascular network (C) from a patient with mild cognitive impairment. The segmentation software removed the large vessel (D, E and F) from the vascular network and extracted the skeletonized microvascular network using processing procedures, such as inverting, equalizing and removing background noise and non-vessel structures to create a binary image (G, H and I). Any vessels with a diameter ≥ 25 μm (D, E and F) were defined as large vessels and were separated from the remaining vessels, which were defined as microvessels. This procedure was also used to eliminate the shadow graphic projection artifact of the large vessels (E) in the superficial vascular plexus on the deep vascular plexus (B). Bar = 0.5 mm.

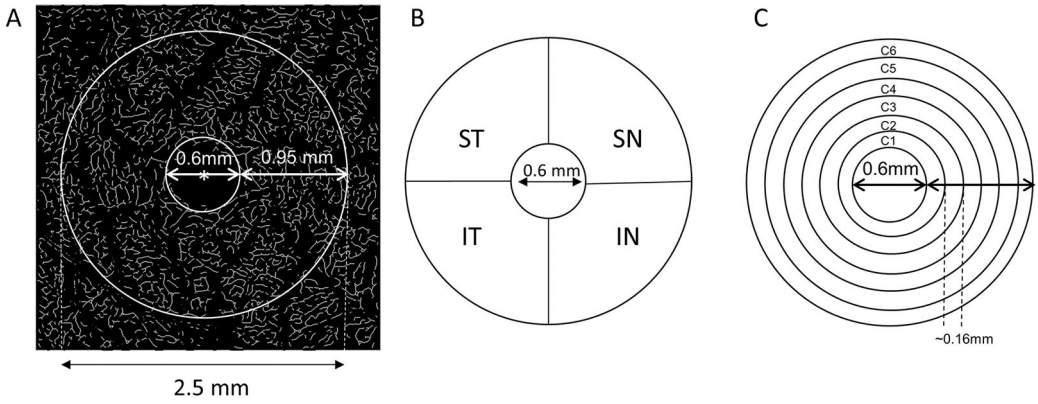

Figure 2. Partitions of the microvascular network

The center (marked as red asterisk*) of the foveal avascular zone (FAZ) was detected in the skeletonized microvasculature image (A) and the center of the FAZ was used to partition the quadrantal and annular zones. The annulus from 0.6 mm to 2.5 mm in diameter was defined as the annular zone with a width of 0.95 mm after removing the avascular zone (diameter = 0.6 mm) centered on the fovea (A). Using the hemispheric partition, the annular zone was then partitioned into four quadrantal sectors (B), named the superior temporal (ST), inferior temporal (IT), superior nasal (SN), and inferior nasal (IN). To analyze the changes in the thin annular zones from the center to the periphery, the annular zone (A) was partitioned into 6 thin annuli named C1 to C6 (D) with a width of ~0.16 mm.

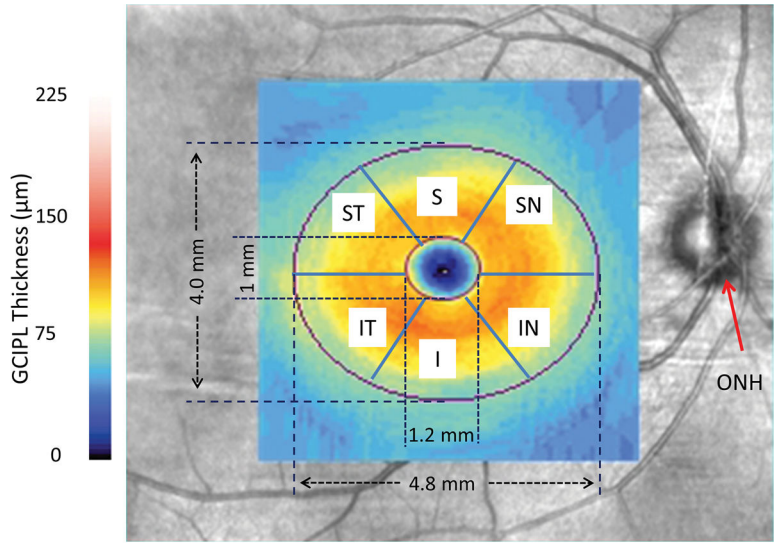

Figure 3. GC-IPL imaging and partition

GC-IPL of the right eye from a patient with mild cognitive impairment was acquired in the macula using Zeiss OCTA and a thickness map was processed in the elliptic annulus with partitions of 6 sectors of the annulus after removal of the central elliptic area. ONH: optic nerve head; ST: superior temporal; S: superior; SN: superior nasal; IN: inferior nasal; I: inferior; and IT: inferior temporal.

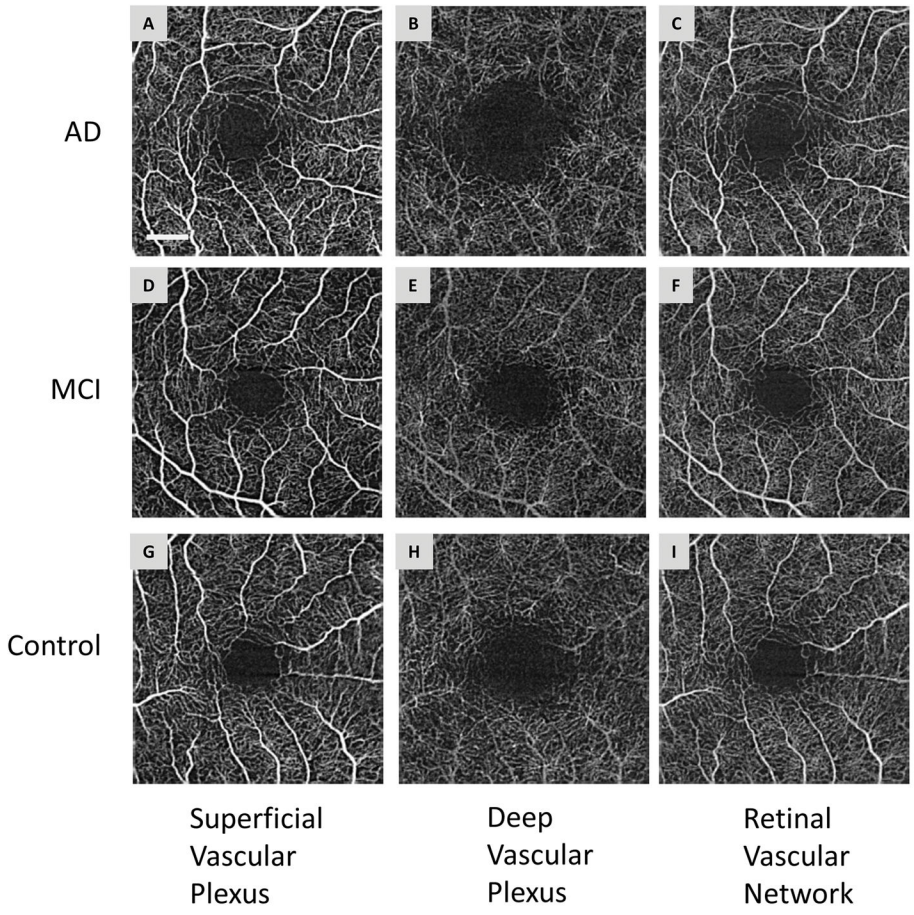

Figure 4. Representative images of the retinal microvascular networks imaged using optical coherence tomography angiography (OCTA)

Patients with Alzheimer disease (AD) (A, B and C) and mild cognitive impairment (MCI) (D, E and F) as well as a control subject (G, H and I) were imaged. Compared to the normal control (G and I), the large vessels in AD and MCI patients had similar densities in the superficial vascular plexus (A and D) and retinal vascular network (C and F) but showed some degrees of tortuosity. The microvessels in the deep vascular plexus in AD (B) and MCI (E) patients appeared to be less dense compared to the normal control (H). Note: the deep vascular plexus images are raw images, showing the graphic projection artifact of the large vessels. Bar = 0.5 mm.